Nakahara, T., and M. Hirata, "The Prediction of Henry's Constants for Hydrogen-Hydrocarbon Systems," *J. Chem. Eng. Jap.*, **2**, 137 (1969).
Neff, R. O., and D. A. McQuarrie, "A Statistical Mechanical Theory of Solubility," *J. Phys. Chem.*, **77**, 4130 (1973).
Pierotti, R. A., "The Solubility of Gases in Liquids," *ibid.*, **67**, 1840 (1963).
Pitzer, K. S., and R. F. Curl, Jr., "Volumetric and Thermodynamic Properties of Fluids—Enthalpy, Free Energy, and Entropy," *Ind. Eng. Chem.*, **50**, 265 (1958).
———., D. Z. Lippman, R. F. Curl, Jr., C. M. Huggins, and D. E. Petersen, "The Volumetric and Thermodynamic Properties of Fluids," *J. Am. Chem. Soc.*, **77**, 3427, 3433 (1955).
Prausnitz, J. M., "Molecular Thermodynamics of Fluid-Phase Equilibria," Prentice-Hall, Englewood Cliffs, N. J. (1969).
———., and P. L. Chueh, "Computer Calculations for High-Pressure Vapor-Liquid Equilibria," *ibid.*, (1968).
———., and R. D. Gunn, "Volumetric Properties of Nonpolar Gaseous Mixtures," *AIChE J.*, **4**, 430 (1958).
Preston, G. T., and J. M. Prausnitz, "A Generalized Correlation for Henry's Constants in Nonpolar Systems," *Ind. Eng. Chem. Fundamentals*, **10**, 389 (1971).
Reamer, H. H., B. H. Sage, and W. N. Lacey, "Volumetric and Phase Behavior of the Methane-n-Heptane System," *J. Chem. Eng. Data*, **1**, 29 (1956).
Reid, R. C., and T. W. Leland, "Pseudocritical Constants," *AIChE J.*, **11**, 228 (1965).
Robinson, R. L., Jr., "Solid-Vapor Equilibrium—A Survey," paper presented at 4th Joint Chem. Eng. Conf., AIChE-Can. Soc. Ch.E., Vancouver (1973).
Shim, J., and J. Kohn, "Multiphase and Volumetric Equilibriums of CH_4-n-Hexane Binary System at Temperatures Between 110° and 150°C," *J. Chem. Eng. Data*, **7**, 3 (1962).
Tee, L. S., S. Gotoh, and W. E. Stewart, "Molecular Parameters for Normal Fluids," *Ind. Eng. Chem. Fundamentals*, **5**, 356, 363 (1966).
Tiepel, E. W., and K. E. Gubbins, "Theory of Gas Solubility in Mixed Solvent Systems," *Can. J. Chem. Eng.*, **50**, 361 (1972).
Yamada, T., "An Improved Generalized Equation of State," *AIChE J.*, **19**, 286 (1973).
Zaalishvili, Sh. E., "Second Virial Coefficients for Gas Solutions," *Z. Fiz. Khim.*, **30**, 1891 (1956).

Manuscript received March 15, 1974; revision received and accepted June 12, 1974.

Fixed Bed Desorption Behavior of Gases with Nonlinear Equilibria:

Part II. Dilute, Multicomponent, Isothermal Systems

Generalized depletion curves for desorption (and corresponding breakthrough curves for adsorption) were calculated for systems characterized by the Langmuir-type multicomponent equilibrium equation and controlled by the film type rate model. In contrast with adsorption where the nonkey (or less strongly adsorbed) component curves display overshoots above feed concentration, in desorption the key component depletion curves exhibit the instabilities in the form of inflections and curvatures. As in the one component case, the differences in the depletion and breakthrough curves may be related to the rate phenomena. The undulations in the key component depletion curves may be characterized by derivatives of the rate data. The major significance of these instabilities is to elongate the depletion curves, which in turn requires the expenditure of added effort during regeneration. Process modifications are indicated, which could suppress the instabilities. The predicted trends were confirmed by experimental depletion curves.

IMRE ZWIEBEL
CHRISTOPHER M. KRALIK
and
JAY J. SCHNITZER

Worcester Polytechnic Institute
Worcester, Massachusetts 01609

SCOPE

Most of the studies dealing with the design of sorption based separation processes have focused on the description of the adsorption step; and even these have been confined mostly to single component systems. From experience, however, the desorption is known to be the controlling step in the operation of the cyclic processes. Recently it was shown that in systems characterized by favorable isotherms ($d^2W/dC^2 < 0$) the depletion curves are considerably elongated in comparison to the corresponding breakthrough curves. Mechanistically the elongation may be

attributed to the nature of the mass transfer driving forces, especially at the latter stages of the desorption step. Such asymmetric behavior requires that a longer time be spent on regeneration than was spent on adsorption. To deal with this problem, special design features have been added to industrial installations; for example, a third bed in the process could provide extra time on desorption, or a temperature/pressure swing step could reduce the time required to regenerate.

Multicomponent systems further complicate the process; for example, during adsorption it is possible to obtain adsorbate concentrations higher than the inlet composition for the nonkey components. (The key component being defined as the component which is adsorbed most strongly). Such overshoots in the composition, referred to as *instabilities*, are the result of the displacement of the nonkey components by the key component. During desorption another type of instability is observed; this time unusual wiggles and waves appear in the key component depletion curves. The characteristics of this instability were the objective of the present study. The prevailing equations describing the system were solved for theoretical solutions, and also experimental measurements were made to observe the behavior of the depletion curves.

The instabilities during the desorption of multicomponent systems manifest themselves as even greater elongations in the depletion curves. To overcome these developments, considerably more complicated design measures have to be implemented than were called for by one component systems if the processes are to be applicable in industrial separations.

CONCLUSIONS AND SIGNIFICANCE

Using the film model to describe the mass transfer mechanism and the Langmuir-type multicomponent isotherm equation to account for nonlinearities in the equilibrium data and for component interactions in the adsorbed phase, both adsorption and desorption profiles were calculated for a broad spectrum of binary mixtures. The relative rate characteristics of the two components were assumed to be identical; thus, emphasis was placed on evaluating the effects of concentration variations, component interactions, and equilibrium characteristics. Thus, in binary systems, four parameters (such as the inlet concentrations C_{i0} and the equilibrium coefficients K_{Li} of both components) can be used to characterize the depletion curves and also the breakthrough curves. With the more strongly adsorbed component defined as the key component, the above can be combined into three characteristic parameters (α_i, the nonlinearity parameters, and η, the relative affinity parameter for the nonkey component).

The nonkey component desorption curves are similar to those obtained in pure component systems. The nonkey component depletion curves do not exhibit an ususual behavior as do the nonkey component breakthrough curves, which overshoot the feed concentration during the adsorption process. The key component depletion curves, on the other hand, exhibit undulations, which have been termed as *instabilities*. These instabilities inadvertently elongate the key component depletion curves in comparison with the corresponding breakthrough curves.

One component desorption could be characterized by the rates of desorption, that is, the first time derivative of the adsorbent loading. In the multicomponent case, due to the component interactions, the instabilities (or wiggles) in the depletion curves require higher order derivatives of the adsorbent loading for the characterization.

When the adsorptive properties of the adsorbing species are quite similar, $\eta \rightarrow 1.0$, no instability occurs regardless of the concentration of either component. When the two adsorbing species are dissimilar in adsorptive properties, $\eta \rightarrow 0$, the instability will appear above a critical composition of the nonkey component. Below this composition the key component behaves as if it was a pure component.

The key component concentrations influence only slightly the appearance of the instabilities. However, the extent of the instability, that is, the extent of the elongation of the depletion curve is a strong function of the key component composition levels.

The experimentally observed nonsymmetrical behavior of adsorption breakthrough curves and desorption depletion curves during one component desorption in fixed beds was interpreted for systems with nonlinear isotherms by Zwiebel et. al. (1972), Garg and Ruthven (1973), and Antonson and Dranoff (1969). Depletion curves, for desorption into an inert purge stream at the same flow rate, temperature, and pressure as in the corresponding adsorption, are considerably elongated in comparison with the corresponding breakthrough curves result from the differences between adsorption and desorption rate phenomena associated with the favorable isotherm. Consequently, a larger time is required to desorb a bed than was spent to accomplish the corresponding saturation. This, automatically, precludes the design of simple cyclic separation processes based upon adsorption. To overcome this deficiency, either a third bed is incorporated in the process, or excess purge gas is used for desorption, or a variety of pressure-swing and/or temperature-swing operations are added. Such costly contributions to the processes confirm the notion that the desorption step is the controlling operation. In spite of this, up to now most of the attention has been devoted to the study of adsorption, with desorption having been described through some simplifying assumptions (Rosen, 1954; Fukunaga et al., 1968).

In multicomponent systems, the interactions between components give rise to instabilities in the gas concentration (Figures 1 and 2) and adsorbent loading profiles which further complicate the relationship between adsorption and desorption. The adsorption of binary systems was initially described by Needham et al. (1966), and in greater detail, using both experimental and theoretical results, by Gariepy and Zwiebel (1971) and by Thomas and Lombardi (1971). In this paper both calculated and experimental depletion curves are presented for binary systems; their behavior is correlated with the isotherm

nonlinearities and related parameters, and they are contrasted with the corresponding breakthrough phenomena.

EXPERIMENT

The results presented here are part of a comprehensive experimental program, parts of which have been previously reported, for example, binary adsorption by Gariepy and Zwiebel (1971), one component desorption by Zwiebel and Schnitzer (1971), and Zwiebel et al. (1972). The apparatus used was described in detail by Gariepy (1972). Using a 180 × 3.75 (I.D.) cm activated charcoal column, dilute binary mixtures of CO_2, C_2H_4, and C_2H_6 in nitrogen were fed during the adsorption step until the adsorbent was completely saturated. Desorption was accomplished by using pure nitrogen purge at the same feed rate and inlet pressure as was used during the corresponding adsorption step. The nitrogen flow rates were varied between 5000 and 15000 s.cc/min. so that the resulting pressure drops were relatively small. The particle based Reynolds numbers, however, were maintained above 1000; that is, all experiments were carried out in the turbulent region. The adsorbate compositions in the gas were kept below 3% total adsorbates to avoid significant velocity effects due to variable flow rate and to minimize thermal effects due to heats of adsorption/desorption. All the experiments were carried out at 25°C, and the temperature of the system was continuously monitored and no significant deviation (less than 1°C) was observed from the ambient initial and inlet conditions. Thus, it may be approximated that the adsorption and desorption experiments were carried out under nearly identical conditions.

Figures 1 and 2 illustrate the experimentally obtained depletion curves, with the specific data describing these experiments given in Table 1. The CO_2 (nonkey component) depletion curves are similar to the curves obtained in the one component case; they are the simple sigmoidal curves, and they very nearly coincide for the cases illustrated. On the other hand, the C_2H_6 (key component) depletion curves exhibit wiggles which inadvertently complicate the desorption step. As the concentration of CO_2 increases in relation to that of C_2H_6 in the feed, the instabilities become more pronounced

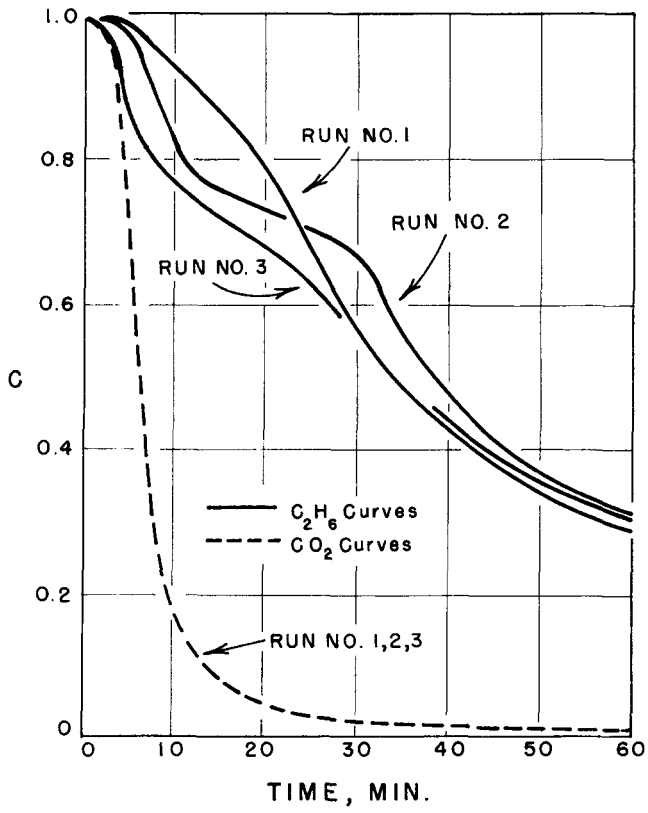

Fig. 1. Experimental depletion curves; different nonkey component (CO_2) concentration levels (see Table 1).

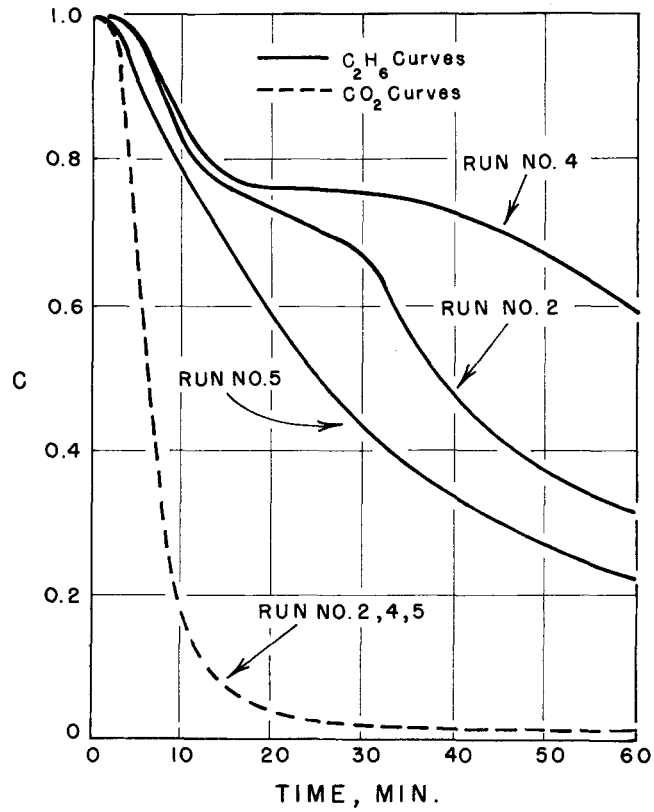

Fig. 2. Experimental depletion curves; different key component (C_2H_6) concentration levels (see Table 1).

Table 1. Component Concentrations During The Adsorbent Loading for the Experimental Runs

Run no. (Figures 1 and 2)	$C_0(C_2H_6)$	$\alpha(C_2H_6)$	$C_0(CO_2)$	$\alpha(CO_2)$	η
	Key component		Nonkey component		
1	0.15	0.5	0.05	0.1	0.33
2	0.15	0.5	0.15	0.3	0.31
3	0.15	0.5	0.25	0.5	0.29
4	0.05	0.16	0.15	0.3	0.23
5	0.25	0.8	0.15	0.3	0.39

C_0 in moles/liter.

(Figure 1), while in the reverse case, at a constant CO_2 composition as the C_2H_6 increases, the ethane depletion curve instabilities become less significant (Figure 2).

ANALYSIS

In analyzing the isothermal adsorption/desorption phenomena of dilute binary systems, the component adsorbate mass balances in the gas phase and in the adsorbent phase may be written as follows:

$$\frac{\partial C_i}{\partial z} + \frac{\partial C_i}{\partial \theta} + A_i \cdot R_i = 0 \qquad (1)$$

$$R_i = \frac{\partial W_i}{\partial \theta} \qquad (2)$$

where the dependent variables C_i and W_i have been normalized with respect to C_{i0} and $W_{i\infty}$, respectively ($W_{i\infty}$ being the multicomponent equilibrium loading of the ith component which corresponds to the gas phase composition C_{i0}).

In this study, the film type of rate expression was used to describe the mass transfer process

$$R_i = \frac{B_i}{A_i}(C_i - C_i^*) \tag{3}$$

This first-order model was selected primarily for its simplicity, thus enabling a convenient means of studying the effects of the equilibrium nonlinearities and component interactions. It was not intended to be a rigorous description of all the rate phenomena, especially for systems with porous adsorbents.

Also, it was stipulated that axial dispersion effects and radial profiles were negligible and that the gas flow rate throughout the column remained constant. The effects of gas phase velocity variation was treated by Zwiebel (1969) and Zwiebel and Schnitzer (1973), the axial dispersion case during adsorption was studied by Ikeda and co-workers (1973), and Lapidus and Almundson (1952), and the effects of particulate internal mass transfer was presented by Garg and Ruthven (1973), Hiester and Vermuelen (1952), and others.

The Langmuir type nonlinear isotherm relationship was chosen to define C_i^*, the normalized gas phase composition in equilibrium with the variable adsorbed phase loading:

$$C_i^* = \frac{W_i}{(1 + \Sigma\alpha_j) - \Sigma\alpha_j W_j} \tag{4}$$

where the nonlinearity parameter $\alpha_i = K_{Li}C_{i0}$, with K_{Li} the Langmuir-type coefficient for the component in question. This expression is quite satisfactory in correlating the equilibrium data over a limited region of adsorbent loadings. However, this does not mean that the system obeys the assumptions of the Langmuir monolayer model.

The boundary conditions for the desorption problem, with a step function elimination of the adsorbate from the feed stream, can be written as follows:

$$C_i(z = 0, \theta) = 0.0 \tag{5a}$$

$$C_i(z, \theta = 0) = F_i(z) = 1.0 \tag{5b}$$

$$W_i(z, \theta = 0) = G_i(z) = 1.0 \tag{5c}$$

Conditions (5b) and (5c) assume that the bed was initially saturated with the adsorbates and that equilibrium was established with the feed gas C_{i0}, which was used in the previous adsorption step.

To obtain analogous solutions to the existing correlations in the literature, a change in variables would have been necessary to give the following independent variables:

$$\text{distance parameters} = B_i \cdot z$$

$$\text{time parameters} = \frac{B_i}{A_i}(\theta - z)$$

This, however, would result in a separate solution for each of the components, with a different abscissa and a different set of parameters for each. To facilitate a more consistent solution whereby the component profiles can be presented together on a single set of coordinates, a key component was defined. In a given system, the component which deviates most from the linear isotherm was chosen as the key component, that is, the one with the largest value of K_{Li}. Consequently, the independent variables were defined as follows:

$$v = B_{\text{key}} \cdot z \tag{6a}$$

$$T = \frac{B_{\text{key}}}{A_{\text{key}}}(\theta - z) \tag{6b}$$

which are similar to those widely used in the literature. For example, v is identical to the column capacity parameter and T/v to the number of transfer units used by Hiester and Vermuelen (1952).

In addition, a relative affinity parameter η_i was defined as

$$\eta_i = \frac{W_{i\infty}/C_{i0}}{W_{k\infty}/C_{k0}} \tag{7}$$

which in terms of the dimensionless coefficients becomes

$$\eta_i = \frac{A_i}{A_{\text{key}}} \tag{7a}$$

The values of this parameter are bracketed, that is, $\eta_i = 0$ indicates that the ith component is not present in the system, and $\eta_i = 1.0$ represents the case where the ith component is adsorbed to the same extent as the key component.

In this study, the relative rates of adsorption of all the components were assumed to be identical, that is, the rate parameter was set at $\phi_i = 1.0$, since emphasis of the comparisons was directed to determine the effects of the relative loadings, the relative isotherm nonlinearities, and the component interactions on the depletion curves.

As a result of the variable changes, the mass balance and mass transfer rate equations were transformed respectively to

$$\frac{\partial C_i}{\partial v} + \eta_i \frac{\partial W_i}{\partial T} = 0 \tag{8}$$

$$\frac{\partial W_i}{\partial T} = \frac{\phi_i}{\eta_i}(C_i - C_i^*) \tag{9}$$

These equations, together with the isotherm equation (4) and the appropriate boundary conditions, represent the multicomponent desorption process. Their solution can provide a set of generalized curves which describe the behavior of systems that conform to the assumptions used in the derivations. As stated above, this system of equations is not intended to be absolutely rigorous for all adsorption/desorption cases. Instead, it is expected to clarify certain interactions and to illustrate the prevailing trends that could be expected as a result of these interactions.

The above system of equations was solved by transforming the partial differential equations into ordinary differential equations along the straight line characteristic curves (Acrivos, 1956)

$$v = \text{constant} \tag{10a}$$

$$T = \text{constant} \tag{10b}$$

The latter were then integrated by a modified Newton's method (Gariepy, 1972) on the DEC PDP-10 computer. An iterative technique was necessitated by the nonlinearities introduced in the denominator of Equation (4).

RESULTS AND DISCUSSIONS

In contrast with the linear single component systems whose description requires one set of curves for each of the two dependent variables, C and W, the multicomponent systems with nonlinear equilibria require a series of sets of curves with different values of the parameters η_i, ϕ_i, and α_i. In all, a system with N adsorbing components requires the specification of $3N - 2$ parameters for complete description (two of the parameters $\eta_{\text{key}} = 1.0$ and $\phi_{\text{key}} = 1.0$ having been set by their definitions). This, in turn, would necessitate a series of generalized plots beyond the capacity of most publications if a broad range of values of all these parameters were to be used in all reasonable combinations. In this paper, typical such data are presented for a binary system, and the previously

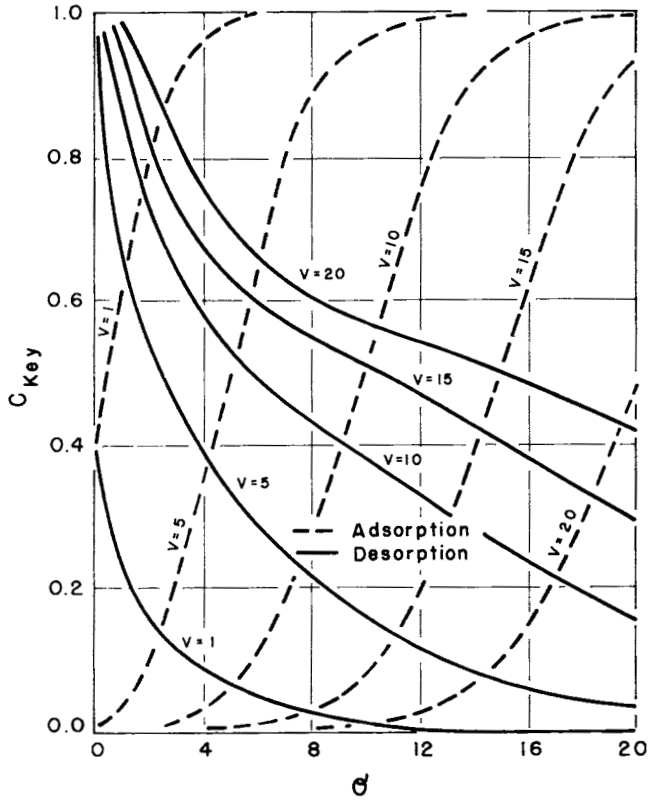

Fig. 3. Calculated gas phase composition profiles for key component; $\alpha_K = 0.9$, $\alpha_{nK} = 0.5$, $\eta = 0.2$.

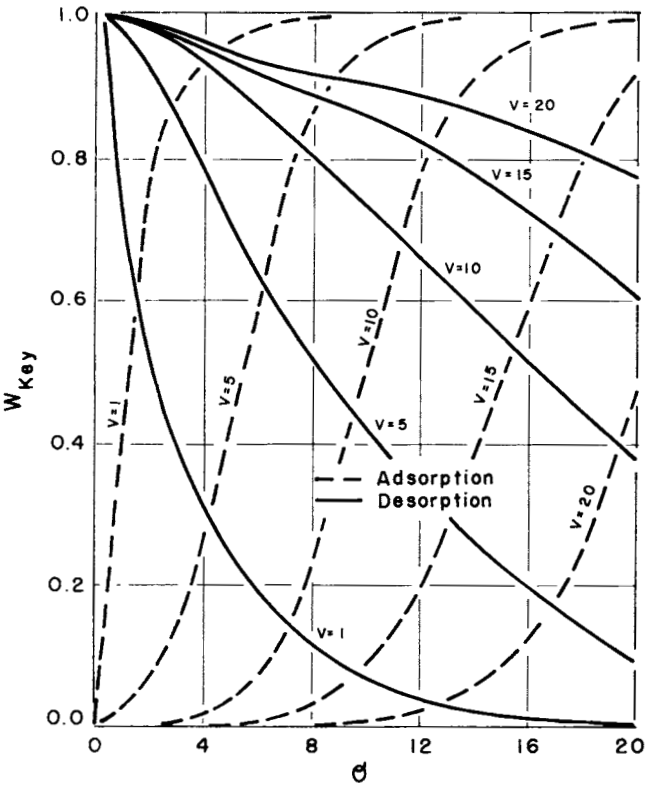

Fig. 4. Calculated adsorbent loading profiles for key component; $\alpha_K = 0.9$, $\alpha_{nK} = 0.5$, $\eta = 0.2$.

mentioned interactions are investigated.

Figures 3 and 4 show typical calculated depletion curves for the key component in the gas and adsorbed phases, respectively. Figure 5 shows the corresponding adsorbent loading curves for the nonkey component. For comparison, these figures also have the corresponding adsorption curves plotted. In contrast to adsorption, where the nonkey component possesses concentration profile anomalies by overshooting the inlet compositions, in desorption the key component profiles exhibit some unusual wiggles. In this paper these wiggles are referred to as *instabilities*. These instabilities appear as a plateauing of the gas concentrations and adsorbent loadings midway through the depletion process.

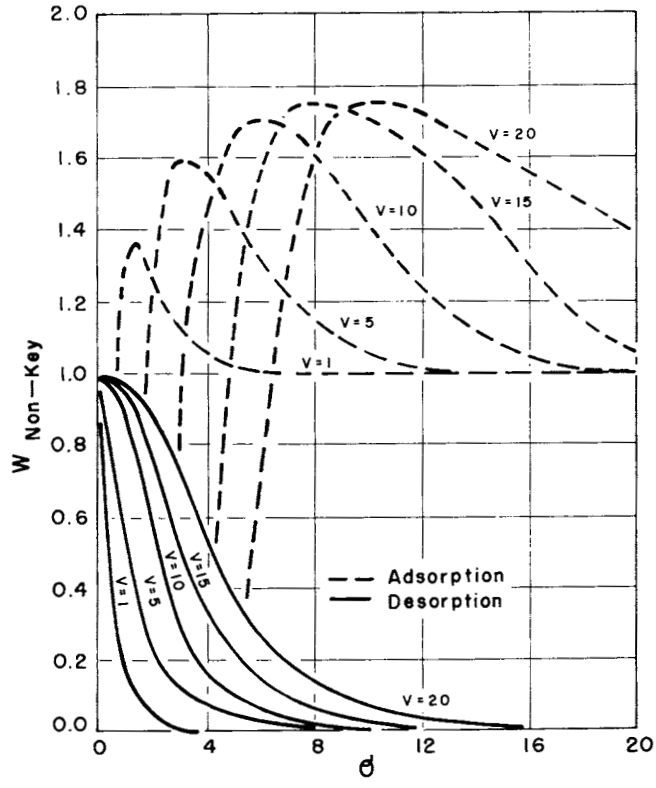

Fig. 5. Calculated adsorbent loading profiles for nonkey component; $\alpha_K = 0.9$, $\alpha_{nK} = 0.5$, $\eta = 0.2$.

The characteristics of the concentration and loading profiles are intimately related to the rates of desorption. The variation of these rates is shown in Figure 6, where the calculated driving forces of the key component, corresponding to the case illustrated in Figures 3 and 4, are plotted as a function of the normalized time. In Figure 7, the rates of desorption at a fixed point in the bed ($v = 10$) are compared for the two components, and they are contrasted with their corresponding adsorption rates. The individual component desorption rates, as in the one component systems (Zwiebel et al., 1972), never reach values as high as the corresponding adsorption rates. Even though initially the desorption rates rise more rapidly, over an extended period the integrated average desorption rates are lower than the corresponding adsorption rates; hence, the elongated depletion curves when they are compared to the corresponding breakthrough curves.

The nonkey component desorption behavior is routine, and it resembles the single component case. On the other hand, the analog to the nonkey component overshoot as a form of instability during the adsorption process is the plateauing of the key component depletion curve during the desorption. In the key component rate curves in a binary system, this phenomenon manifests itself as a rate function with two peaks. The first one occurring at the same time as the nonkey desorption rate peak, the second

one somewhat later, after essentially all the nonkey has been desorbed.

In considering the effects on the desorption rates, the relative influence of the three variables appearing in the driving force portion of the rate equation must be analyzed. For example, as can be seen from the following expression:

$$|C_k - C_k^*| = \frac{W_k}{(1 + \alpha_k + \alpha_{nk}) - \alpha_k W_k - \alpha_{nk} W_{nk}} - C_k \tag{10}$$

the key component desorption driving force is directly affected by the key component adsorbent loading; that is, as W_k decreases, the magnitude of the driving force $|C_k - C_k^*|$ decreases since C_k^* decreases. This is a relatively strong effect because the numerator of C_k^* decreases and denominator increases as W_k decreases. The effects of the pertinent variables on the desorption rate are summarized in Table 2. Consequently, the first peak in the key component rate curve is primarily the result of rapid initial decrease in C_k. The changes in W_k and W_{nk} at this early stage in the run ($\theta < 1.5$) are relatively small to contribute significantly to the desorption rate of the key component.

The decrease in the key component desorption rate, that is, the descent towards the valley in the rate curve, is caused by the combination of three effects; the decreasing slope of the C_k vs. θ curve, and the decreasing values of both W_k and W_{nk}. The decreasing values of W_k and W_{nk} are the expected desorptive effects; however, the changing slope of the C_k curve is the result of an effective accumulation of key component in the gas phase.

Once the nonkey component adsorbent loading reaches relatively low values ($W_{nk} < 0.2$), the process becomes essentially a one component desorption. From thereon, the relative values of W_k (in C_k^*) and C_k are such that the rate of desorption rises to the second peak. This peak is rather low and broad, resulting in a slow desorption of the key component and contributing to the elongation of the desorption well beyond the time required to saturate the bed.

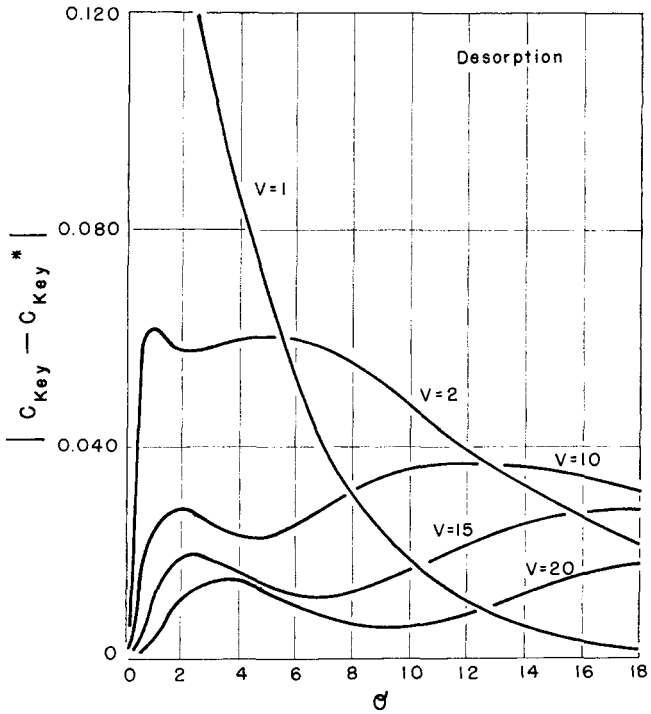

Fig. 6. Desorption rate profiles for key component $\alpha_K = 0.9$, $\alpha_{nK} = 0.5$, $\eta = 0.2$.

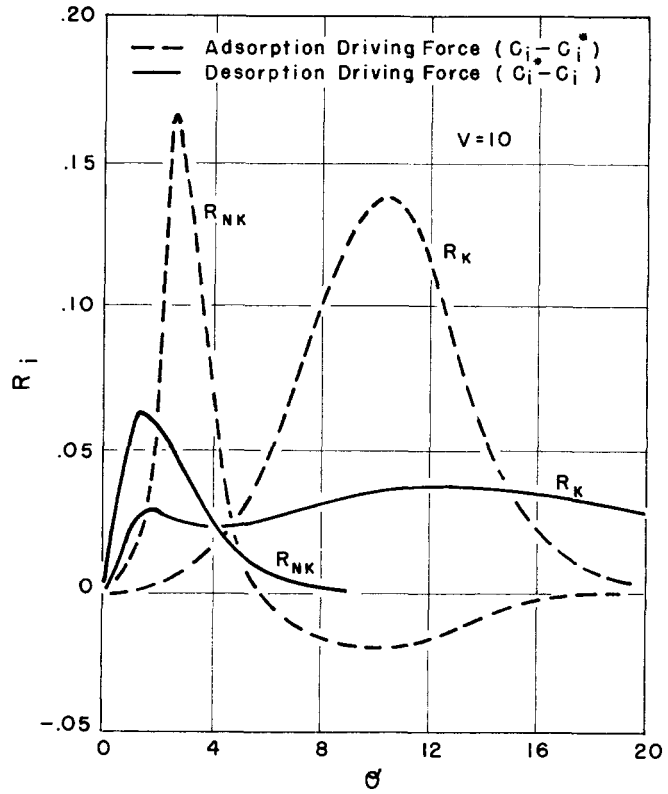

Fig. 7. Comparison of adsorption and desorption driving forces.

TABLE 2. VARIABLES AFFECTING THE DRIVING FORCES

Variables	$\lvert C_k - C_k^* \rvert$	$\lvert C_{nk} - C_{nk}^* \rvert$
C_k	Inverse	No effect
W_{nk}	Strong direct	Moderate effect
C_{nk}	No effect	Inverse
W_k	Moderate direct	Strong direct

The rather complex path followed by the key component during both the adsorption and desorption processes is illustrated in Figure 8. Here, along the three-dimensional representation of the equilibrium surface the operating paths are drawn. The heavy curves represent both the operating curve and the corresponding equilibrium curve. The separation between the two is so small that they could not be distinguished on the scale of Figure 8. The complex route traversed during the desorption process gives rise to the development of the instabilities.

CORRELATIONS

The distinctive features of the key component depletion instability are best identified by analyzing the derivatives of the desorption rate, that is, the second derivatives of the adsorbent loading profiles:

$$\frac{\partial R_i}{\partial \theta} = \frac{\partial^2 W_i}{\partial \theta^2} \tag{11}$$

or

$$\frac{\partial R_i}{\partial \theta} = \frac{B_i}{A_i}\left(\frac{\partial C_i}{\partial \theta} - \frac{\partial C_i^*}{\partial \theta}\right) \tag{12}$$

Differentiating Equation (4) and substituting into Equation (12) gives

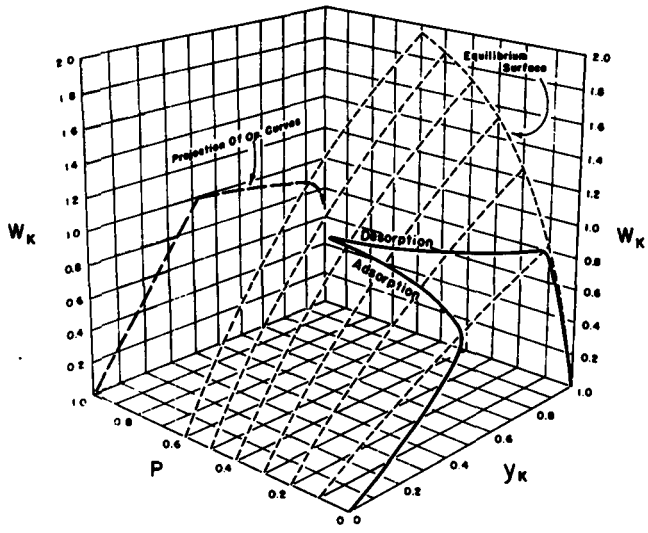

Fig. 8. Operating curves during adsorption and desorption superimposed on equilibrium surface. Equilibrium paths coincide with operating curves.

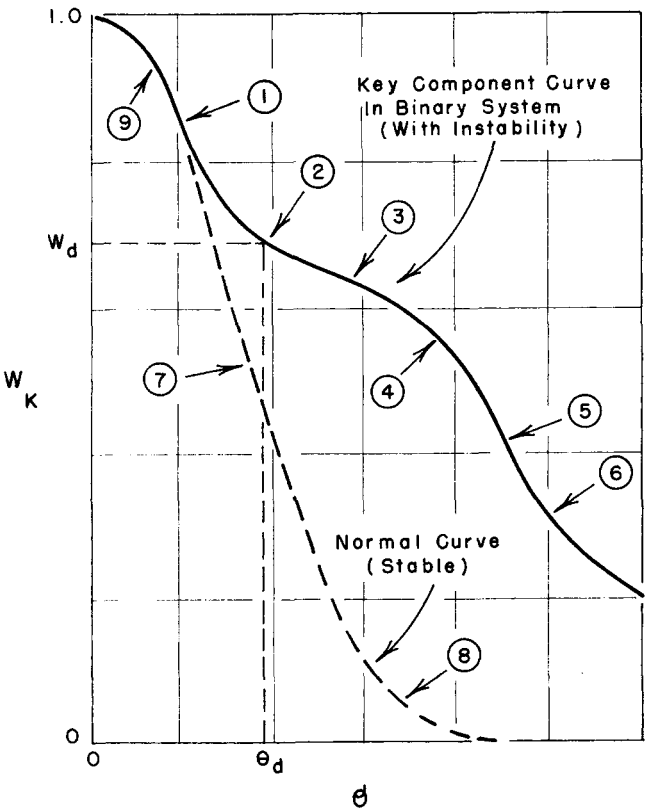

Fig. 9. Schematic depletion curves with characteristic points illustrating instability.

$$\frac{\partial^2 W_i}{\partial \theta^2} = \frac{B_i}{A_i}\left\{\frac{\partial C_i}{\partial \theta} - \frac{C_i^*}{W_i}\left[R_i + C_i^* \sum_{j=1}^{N} \alpha_j R_j\right]\right\} \quad (13)$$

which for the key component in a binary sorbate system becomes

$$\frac{\partial^2 W_k}{\partial \theta^2} = \frac{B_k}{A_k}\left\{\frac{\partial C_k}{\partial \theta} - \frac{C_k^*}{W_k}[R_k(1 + \alpha_k C_k^*) + C_k^* \alpha_{nK} R_{nK}]\right\} \quad (14)$$

The zeros of the second derivative function correspond to the peaks and valleys of the rate curve, or the inflection points on the adsorbent loading curve (points 1, 3, and 5 on Figure 9). The maxima and minima of the second derivative function correspond to the points of maximum curvature on the adsorbent loading curve (points 2, 4, 6, and 9 on Figure 9). (This latter correspondence is only approximate, but quite satisfactory because $(\partial W_i/\partial\theta)^2 << 1.0$.) The normal, or stable depletion curve, also shown on Figure 9, typical of one component desorption, possesses only two points of maximum curvature (points 8 and 9) and one point of inflection (point 7).

The early appearance of the inflection point (point 1 as contrasted with point 7 on Figure 9) results in a departure from the normal monotonic depletion curve. The two inflection points, points 1 and 3, and the two regions of curvature, near points 2 and 4, constitute the instability in the key component depletion curve. The final inflection point and the final region of curvature (point 5 and the vicinity of point 6, respectively), may be viewed as the counterparts to the similar points on the stable curve (points 7 and 8). Usually the last two points on the unstable curves occur after the nonkey component has been completely desorbed, that is, they correspond to pure component desorption.

The second derivative function is an implicit cubic equation in W_k and $\partial C_k/\partial\theta$ so that an analytic solution is not readily available. However, the second derivatives can be evaluated routinely during the numerical integration of the original model equations. Figure 10 gives the second derivative profiles of the key component for the illustrated case. The locations of the peaks and valleys of the rate curves are clearly spotted by the zeros of the second derivative curve, and the points of maximum curvature in the adsorbate loading profile are also readily identified by the peaks (positive and negative) of the second derivative function. These correlations utilizing the second derivative functions suggest the existence of

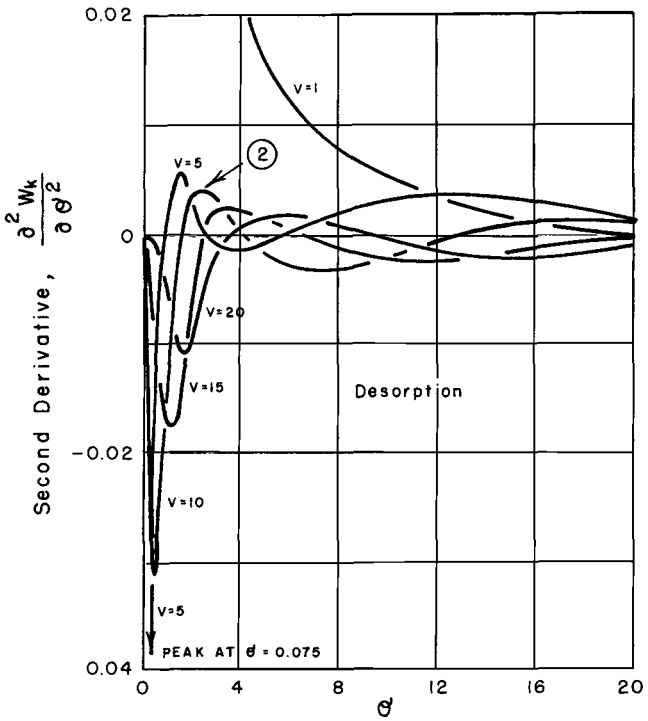

Fig. 10. Second derivative profiles of depletion curves; $\alpha_K = 0.9$, $\alpha_{nK} = 0.5$, $\eta = 0.2$.

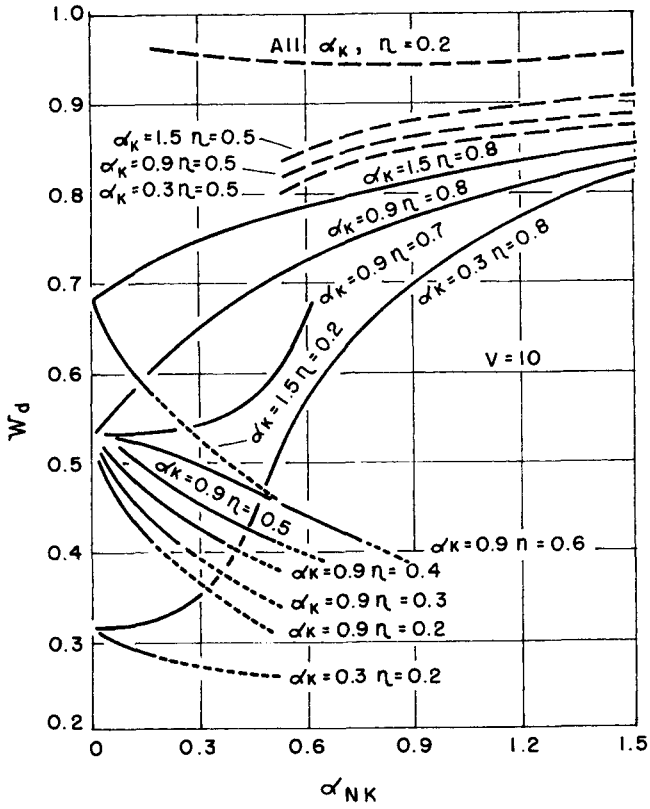

Fig. 11. Location of upper concave curvature characterizing key component instability.

significant diffusive mechanisms in the multicomponent desorption case, which are absent in pure component desorption.

In this paper, for the description and correlation of the instabilities the value of W_d (Figure 9) was selected as the characteristic variable. It is the adsorbent loading at the point of maximum curvature in the upper concave curved region (near point 2), corresponding in time to the first maximum in the second derivative function (Figure 10). This choice was arbitrary; similar results could be obtained if either of the coordinates (W or θ) at any one of the characteristic points, (points 1, 2, 3, and 4), or for that matter the values of the first or second derivatives at one of these points had been chosen.

In Figure 11 the characteristic values of W_d are plotted as a function of α_K, α_{nk}, and η_{nk}. (For binary systems the affinity parameter for the nonkey component η_{nK} may be written without subscript η since $\eta_K = 1$). The curves with low values of the relative affinity parameter η become discontinuous at a critical value of α_{nK}^*. At α_{nK} lower than α_{nK}^*, that is, at low concentrations of the nonkey component, there is only one region of concave curvature, and no instability is observed. At the critical value of α_{nK}^* the instabilities appear at rather high values of the adsorbent loading (for example, with $\eta = 0.2$ the value of $\alpha_{nK}^* = 0.17$ and the instability occurs at $W_K > 0.9$), and thereafter the location of the upper concave curvature is given by the nearly horizontal upper branch of the characterization curve (dashed lines). The tendency for instability is reinforced by the fact that the two components have dissimilar adsorptive properties at low values of η. However, low values of α_{nK} correspond to low nonkey component concentration levels where the key component behaves essentially independently, hence the stable regions. This trend was illustrated experimentally on Figure 1, where Run 1 exhibits a stable depletion curve, but Runs 2 and 3 [at increasing values of $\alpha(CO_2)$] show instabilities.

It is noteworthy that in cases where instability does occur the location of the lowest point of maximum curvature (point 6 on Figure 9) falls along the extension of the stable branch of the characterization curve. (See dotted sections on Figure 11.) Confirming the stipulation that this point represents a return to the stable regime.

At a fixed nonkey component concentration (α_{nK} = constant), increasing the key component concentration (increasing α_K) will not affect significantly the location of the start of the instability (see Figure 11, the dashed lines are very close to each other), but will sharpen the depletion curves. This is in agreement with the pure component analysis of Zwiebel et al. (1972) which showed that increased concentration levels relatively reduced the time required for desorption. This trend was also confirmed experimentally, as shown on Figure 2.

As the value of η increases, that is, as the nonkey component adsorptive properties become more like those of the key component, the instabilities will appear at higher nonkey compositions (α_{nK}^* increases). In fact, at sufficiently high values of η no instabilities occur regardless of the composition of either component. The critical value of η, above which no instabilities occur, appears to be at $\eta \approx 0.68$, where the value of α_{nK}^* asymptotically approaches infinity (See Figure 12). This indicates that very high nonkey component concentrations are required for instability. The curve in Figure 12 establishes the boundary between the stable and unstable regions of a binary desorption system.

SUMMARY

The instability in the key component depletion curve of a multicomponent desorption system was identified and its characteristics were correlated. The instabilities contribute

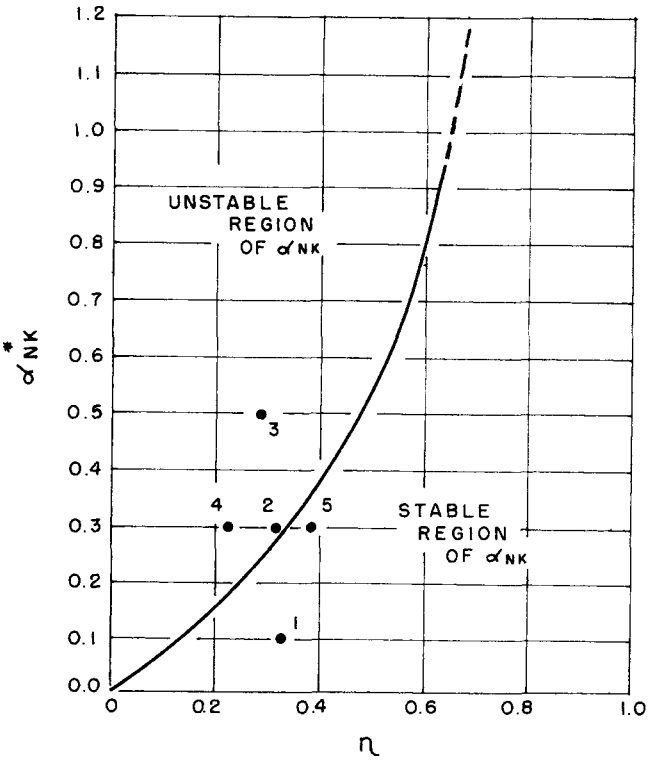

Fig. 12. Key component instability characteristic curve, separating stable and unstable regions. Numbers along points correspond to run numbers of Table 1.

to the elongation of the depletion curves, and this represents an economic disadvantage when cyclic separation units are being designed. The instabilities predominate when the adsorptive properties of the two components are unlike (low values of the relative affinity parameter η) and when the nonkey component is present at relatively high concentrations (high values of α_{nK}).

To overcome the design complications caused by these instabilities it becomes desirable to evaluate alternate desorption conditions. For example, the heretofore often used procedure of heating the beds to increase desorption rates may prove to be an added advantage in that the equilibria of the components are equalized at the elevated temperatures and thus the value of η is increased. Other alternatives may include the use of large quantities of purge gas so that the concentrations of the nonkey component are reduced below the critical value ($\alpha_{nK} < \alpha_{nK}^*$) and thus shifting the system into the stable operating region. Such remedies, however, may present other problems, for example, broadened depletion curves, high velocities with increased pressure drops and excessively dilute desorbate. Regardless of the alternate measures selected to improve the desorption process, added cost factors have to be realized, which indicates that careful systems optimization must be incorporated into the designs.

ACKNOWLEDGMENT

The authors gratefully acknowledge the support of the National Science Foundation. Also, they appreciate the assistance of Mr. Charles A. Keisling and Mrs. Norma Jacob in the preparation of the manuscript.

NOTATION

A_i = dimensionless capacity coefficient $= \rho_B/fK_i$
B_i = dimensionless rate coefficient $= k_iL/V$
c_i = gas phase composition of i-th component, moles/volume
C_i = normalized gas phase composition $= c_i/C_{i0}$
C_i^* = normalized equilibrium gas phase composition, see Equation (4)
C_{i0} = inlet gas phase composition to adsorption step, moles/volume
f = void fraction of bed, volume void/bed volume
$F_i(z)$ = initial normalized gas phase composition distribution along the length of the column
$G_i(z)$ = initial normalized adsorbed phase loading distribution along the length of the column
k_i = mass transfer coefficient, moles/time/bed volume/concentration
K_i = $C_{i0}/W_{i\infty}$, concentration-capacity ratio of feed, mass/volume
K_{Li} = equilibrium coefficient, (moles/volume)$^{-1}$
L = bed length, for example in cm
N = total number of adsorbing components
P = partial pressure of adsorbates in gas stream containing inert carrier (see Figure 8)
R_i = rate of mass transfer between phases, see Equation (3)
t = time, for example in min.
T = dimensionless time parameter, see Equation (6b)
v = dimensionless distance parameter, see Equation (6a)
V = constant superficial gas phase velocity, volumes/time
w_i = adsorbed phase loading of the ith component, moles/adsorbent mass
$W_{i\infty}$ = adsorbed phase loading in equilibrium with inlet gas phase composition, moles/adsorbent mass
W_i = normalized adsorbed phase loading, $w_i/W_{i\infty}$
x = axial position, for example in cm
Y_i = gas phase mole fraction of ith component
z = normalized axial position $= x/L$

Greek Letters

α = nonlinearity parameter $= K_{Li}C_{i0}$
α^*_{nK} = critical value of non-key component non-linearity parameter
η_i = dimensionless relative affinity parameter, see Equation (7)
η = dimensionless relative affinity parameter of nonkey component in binary adsorption system $= \eta_{nK}$
θ = normalized time $= Vt/fL$
ρ_B = bulk density of column, adsorbent mass/bed volume
ϕ_i = relative rate coefficient $= B_i/B_k$

Subscripts

i = component species i
j = dummy component species in summation terms
k = key component
nK = nonkey component

LITERATURE CITED

Acrivos, Andreas, "Method of Characteristics Technique," *Ind. Eng. Chem.*, **48**, 703 (1956).

Antonson, C. R., and J. S. Dranoff, "Non-linear Equilibrium and Particle Shape Effects in Intraparticle Diffusion Controlled Adsorption," paper presented at the 64th National AIChE Meeting, New Orleans (1969).

Fukunaga, Paul, K. C. Hwang, S. H. Davis and J. Winnick, "Mixed-Gas Adsorption and Vacuum Desorption of Carbon Dioxide on Molecular Sieve," *Ind. Eng. Chem. Process Design Develop.*, **7**, 269 (1968).

Garg, D. R., and D. M. Ruthven, "Theoretical Prediction of Breakthrough Curves for Molecular Sieve Adsorption Columns," *Chem. Eng. Sci.*, **28**, 799 (1973).

Gariepy, R. L., "Dynamic Behavior of Gas Mixtures in Fixed Bed Adsorption Columns," Doctoral thesis, Worcester Polytechnic Inst., Mass. (1972).

———., and I. Zwiebel, "Adsorption of Binary Mixtures in Fixed Beds," *AIChE Symp. Ser., No. 117*, **67**, 17 (1971).

Hiester, N. K., and T. Vermuelen, "Saturation Performance of Ion Exchange and Adsorption Columns," *Chem. Eng. Progr.*, **48**, 505 (1952).

Ikeda, K., H. Ohya, O. Kanemitsu, and K. Shimomura, "La Curbe De Percee De L'Adsorption En Lit Pour Une Isotherm Favorible," *Chem. Eng. Sci.*, **8**, 227 (1973).

Lapidus, Leon, and N. R. Amundson, "Mathematics of Adsorption in Beds. VI. Effect of Longitudinal Diffusion in Columns," *J. Phys. Chem.*, **56**, 984 (1952).

Needham, R. B., J. M. Campbell, and H. O. McLeod, "Critical Evaluation of Mathematical Models Used for Dynamic Adsorption of Hydrocarbons," *Ind. Eng. Chem. Process Design Develop.*, **5**, 122(1966).

Rosen, J. B., "Kinetics of a Fixed Bed System for Solid Diffusion Into Spherical Particles," *Ind. Eng. Chem.*, **46**, 1590 (1954).

Thomas, W. J., and J. L. Lombardi, "Binary Adsorption of Benzene-Toluene Mixtures," *Trans. Inst. Chem. Engrs.*, **49**, 240 (1971).

Zwiebel, Imre, "Fixed Bed Adsorption with Variable Gas Velocity due to Pressure Drop," *Ind. Eng. Chem. Fundamentals*, **8**, 803 (1969).

———., R. L. Gariepy and J. J. Schnitzer, "Fixed Bed Desorption Behavior of Gases with Non-Linear Equilibria: Part I. Dilute, One Component, Isothermal Systems," *AIChE J.*, **18**, 1139 (1972).

Zwiebel, Imre, and J. J. Schnitzer, "Desorption from Fixed Bed Columns Containing Activated Carbon," paper presented at 10th Intern. Carbon Conf., Bethlehem, Pa. (1971).

———., "Desorption from Fixed Beds," paper presented at 74th National AIChE Meeting, New Orleans (1973).

Manuscript received February 11, 1974; revision received May 20 and accepted May 21, 1974.